Δελτίο της Ελληνικής Γεωλογικής Εταιρίας, τόμος L, σελ. 392-401
Πρακτικά 14ου Διεθνούς Συνεδρίου, Θεσσαλονίκη, Μάιος 2016

Bulletin of the Geological Society of Greece, vol. L, p. 392-401
Proceedings of the 14th International Congress, Thessaloniki, May 2016

APPLICATION OF OSL METHOD IN DATING PAST EARTHQUAKES

Tsodoulos I.[1], Stamoulis K.C.[1,2], Papachristodoulou C.[1], Pavlides S.[3] and Ioannides K.G.[1,2]

[1]*University of Ioannina, Department of Physics, 45110, Ioannina, Greece, itsodoul@cc.uoi.gr, kstamoul@cc.uoi.gr, xpapaxri@cc.uoi.gr, kioannid@cc.uoi.gr*

[2]*Archaeometry Center, University of Ioannina, 45110, Ioannina, Greece, kstamoul@cc.uoi.gr*

[3]*Aristotle University of Thessaloniki, Department of Geology, 54124, Thessaloniki, Greece, pavlides@geo.auth.gr*

Abstract

The aim of this study was to establish a chronological frame of paleoseismic events of Gyrtoni Fault, (Thessaly, Central Greece), with the use of OSL dating method. The Gyrtoni Fault, defines the north-eastern boundary of the Middle-Late Quaternary Tyrnavos Basin, and was previously investigated with geological methods. Twenty five fluvial-colluvial sediment and pottery samples were collected from two paleoseismological trenches, excavated along the Gyrtoni Fault, from both the upthrown and the downthrown fault blocks. Optically Stimulated Luminescence (OSL) dating was applied to coarse grain quartz using the single-aliquot regenerative-dose (SAR) protocol. Investigations of luminescence characteristics using various tests confirmed the suitability of the material for OSL dating using the SAR protocol. Radioactivity measurements were performed in order to estimate the annual dose rate of the surrounding soils to which the quartz grains were submitted during the burial period of the collected samples. The estimated OSL ages agreed well with the available stratigraphical data, and archaeological evidence. The occurrence of three surface faulting events in a time span between 1.42 ± 0.06 ka and 5.59 ± 0.13 ka was revealed while an earlier faulting event (fourth) was also recognized to be older than 5.59 ± 0.13 ka.
Keywords: *OSL dating, SAR protocol, annual dose rate, paleoseismology.*

Περίληψη

Σκοπός αυτής της μελέτης ήταν να δημιουργήσει ένα χρονολογικό πλαίσιο των παλαιοσεισμών στο ρήγμα Γυρτώνης, (Θεσσαλία, Κεντρική Ελλάδα), με τη χρήση της μεθόδου χρονολόγησης OSL. Το ρήγμα Γυρτώνης, ορίζει το βόρειο-ανατολικό όριο της Λεκάνης Τυρνάβου, και έχει ερευνηθεί στο παρελθόν με γεωλογικές μεθόδους. Είκοσι πέντε δείγματα ιζημάτων, ποτάμιας-κολλουβιακής προέλευσης και κεραμικά δείγματα συλλέχθηκαν από δύο παλαιοσεισμολογικές τάφρους, κατά μήκος του ρήγματος Γυρτώνης, τόσο από το ανερχόμενο όσο και από το κατερχόμενο τέμαχος του ρήγματος. Η μέθοδος της οπτικά προτρεπόμενης φωταύγειας (OSL) χρησιμοποιήθηκε για τη χρονολόγηση κόκκων χαλαζία σύμφωνα με το πρωτόκολλο αναγεννόμενης δόσης μεμονωμένου δισκίου (SAR). Η έρευνα των χαρακτηριστικών φωταύγειας, επιβεβαίωσε την καταλληλότητα του υλικού για χρονολόγηση με τη μέθοδο OSL, χρησιμοποιώντας

το πρωτόκολλο SAR. Μετρήσεις ραδιενέργειας διενεργήθηκαν για την εκτίμηση του ετήσιου ρυθμού δόσης των εδαφών στον οποίο υποβλήθηκαν οι κόκκοι χαλαζία κατά τη διάρκεια της περιόδου ταφής των δειγμάτων. Οι εκτιμώμενες ηλικίες συμφωνούν επίσης με τα διαθέσιμα στρωματογραφικά, και αρχαιολογικά δεδομένα. Από τη συνεκτίμηση στρωματογραφικών δεδομένων και του χρονολογικού πλαισίου προέκυψαν τρία σεισμικά γεγονότα σε ένα χρονικό διάστημα μεταξύ 1.42 ± 0.06 ka και 5.59 ± 0.13 ka ενώ επίσης εκτιμήθηκε ένα παλαιότερο σεισμικό γεγονός (τέταρτο) με πιθανή ηλικία μεγαλύτερη από 5.59 ± 0.13 ka.
Λέξεις κλειδιά: *OSL dating, SAR protocol, annual dose rate, paleoseismology.*

1. Introduction

The Gyrtoni Fault (GF), a south-dipping normal fault affecting Thessaly, Central Greece (Pavlides *et al.*, 2010), is located ~13 km from Larissa, one of the largest cities of Greece (population ~160.000, Fig. 1). Therefore, the understanding of the seismotectonic behavior of this active fault in terms of slip rate, recurrence interval and date of past earthquakes (McCalpin, 2009b), is of great importance considering the hazard due to a future great seismic event for the population of the area.

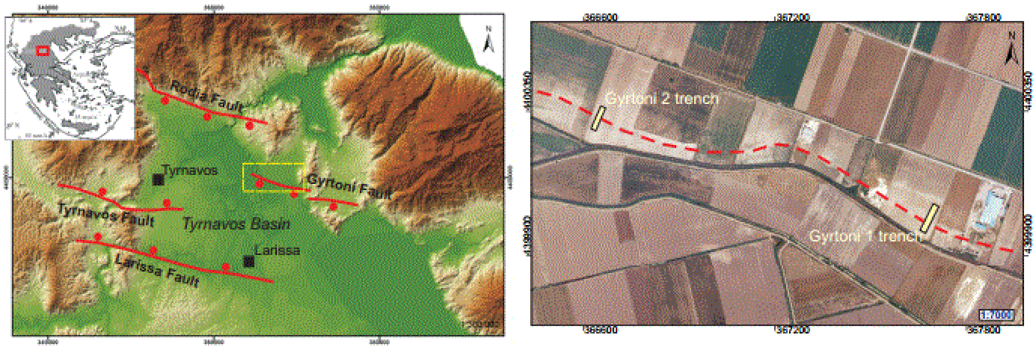

Figure 1 - a) Digital Elevation Model with hill-shading relief of the Tyrnavos Basin showing the main structural features. b) Simplified geological map of the study area, and the locations of the two trenches. Images taken form Google Earth.

Several large events have occurred in Thessaly during historical times and the instrumental period (Caputo *et al.*, 2006 and references therein), but only three of these events have been directly related to the Tyrnavos Basin; the 1731 (Ms 6.0), the 1781 (Ms 6.3) and the 1941 (Ms 6.1) earthquakes (Papazachos and Papazachou, 1997). Also, archaeological data, based on remains and damaged monuments, provide evidence of strong earthquakes in the Tyrnavos Basin during the last 2-3 ka (Caputo and Helly, 2005b). However, the correlation of these events with specific faults of Tyrnavos Basin is still under discussion.

Optically Stimulated Luminescence (OSL) dating (Huntley *et al.*, 1985) provides age estimates for the last time a sediment was exposed to sunlight and is a potentially useful tool in dating earthquake-related deposits (e.g. Aitken, 1998). The single-aliquot regenerative-dose (SAR) protocol (Murray and Wintle, 2003) is extensively used for measuring the equivalent dose (D_e), providing a high degree of precision and accuracy for OSL ages (Murray and Olley, 2002). OSL dating studies based on the SAR protocol applied to date earthquake-related deposits provide reliable results (Porat *et al.*, 1996; Chen *et al.*, 2003; Fattahi *et al.*, 2010).

Only a few previous studies have applied luminescence dating to fault-related deposits associated with paleoerthquakes, in Greece. Chatzipetros *et al.* (1998) were the first to apply thermoluminescence (TL) and ^{14}C dating to colluvial sediments associated with the Palaeochori-Sarakina Fault in western Macedonia, Greece, for estimating recurrence intervals of past earthquakes.

In palaeoseismological investigations carried out along the Tyrnavos and the Rodia faults, Central Greece, Caputo *et al.* (2004) and Caputo and Helly (2005a) reported TL, OSL and AMS ages from numerous trenches and quantified the most important seismotectonic parameters.

In the present study, chemically purified quartz extracted from fluvial-colluvial sediment and pottery samples, which were collected from two excavated paleoseismological trenches along the GF, was subjected to OSL dating method using the SAR protocol (Murray and Wintle, 2003). The chronological determination of the identified past surface faulting events has been constrained by the obtained OSL ages of the observed stratigraphic units. Our results allowed the estimation of the Holocene slip rate, the mean return period and the elapsed time from the last earthquake on the GF. In addition, the establishment of a reliable chronological framework for the floodplain deposits exposed in the excavated trenches was employed.

2. Materials and Methods

2.1. Sample collection

To establish a reliable chronological framework for this area, six samples for OSL dating were collected from four of the five distinct lithologic units exposed on the upthrown fault block of an excavated trench G1, perpendicular to the Gyrtoni Fault. Additionally, three samples were collected from fallen blocks belonging to another fifth unit and involved in the shear zone. To evaluate internal consistency, also three samples were collected from the exposed units of the upthrown fault block of a second excavated trench G2. Eight sediment samples and five pottery fragments were collected from the four distinct lithologic units exposed on the downthrown fault blocks of the two trenches to constrain the timing of the earthquake events observed in the trenches and thus reconstruct the recent seismotectonic behavior. One sediment sample and four pottery fragments, as well as pieces from buried pottery were collected from silty clay units of trench G1. Due to the lack of clear layering and some uncertainty in the recognition of the units of trench G2, four samples were collected in a vertical sequence in order to establish an age trend with depth (McCalpin, 2009a), and two from different parts close to the fault zone of the fifth unit from trench G2. One additional sample was collected from the silty sand colluvial deposit unit that was exposed on the west wall of the same trench. For details on litholigical units of the two trenches, see Tsodoulos *et al.* (2016).

All sediment samples were collected by hammering 20 x 5 cm steel tubes horizontally into the surface of the walls of the two trenches, which were then carefully dragged out. The tubes were closed and sealed using duct tape and aluminum foil, labeled and stored in black plastic bags. Also, an additional sample for water content estimation and dose rate determination was collected.

2.2. Sample preparation

Sample preparation and luminescence measurements were carried out at the luminescence dating laboratory of the Archaeometry Center at the University of Ioannina. The collected steel tubes were opened under subdued red light laboratory conditions. The outermost 2 cm of the sediment were removed from each end of the steel tubes to avoid contamination with light-exposed material and then the sediment from the central part of the cores was reserved for quartz OSL equivalent-dose (D_e) determination. Pottery samples were sawed with a low speed diamond-impregnated wheel in order to remove a 2 mm layer from the surface and then were gently crushed and grinded using a vice and a mortar. The grain-size fraction of 125-250 μm, for samples from trench G1, and 63-100 μm, for samples from trench G2, were extracted by wet-sieving. The extracted grains were treated with 8% HCl and 30% H_2O_2 to remove carbonates and organic material. Finally, 40% HF was applied for 1 h to remove feldspars and to etch the outer surface of quartz grains, thus eliminating the alpha contribution, followed by concentrated HCl to remove any remaining soluble fluorides. After the chemical treatment, the grains were mounted on 10 mm diameter stainless steel discs by evaporation of an acetone suspension. The purity of the quartz extract was checked using the OSL-

IR depletion ratio with an extra step within the SAR sequence (Duller, 2003) and by observing the 110 °C TL peak during preheating (Constantin *et al.*, 2014). (Fig. 2).

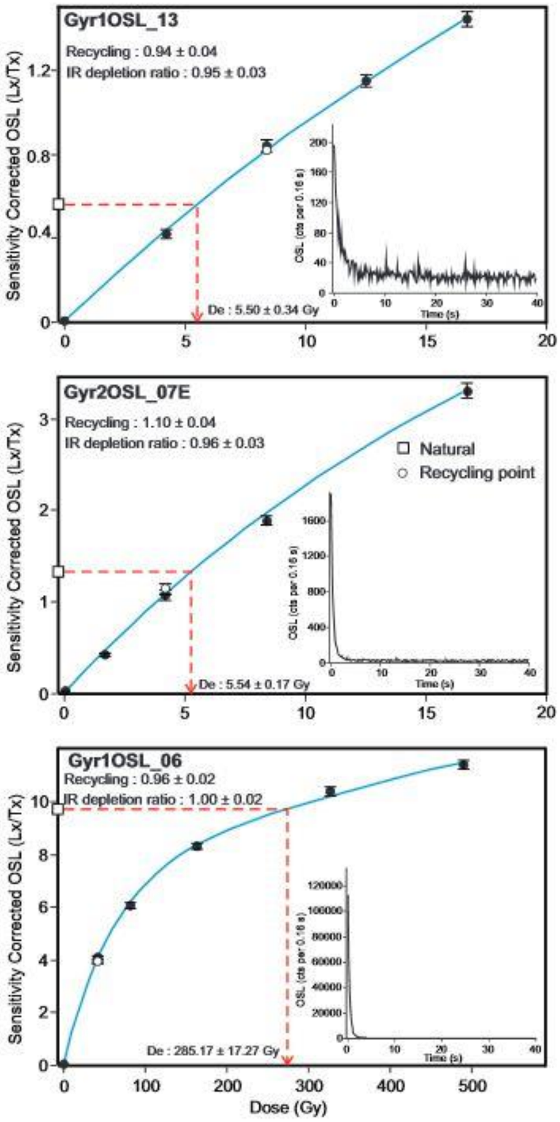

Figure 2 - Typical OSL decay curves (inset) and SAR growth curves for pottery (Gyr1OSL_13) and sediment (Gyr2OSL_07E and Gyr1OSL_06) samples using a 260ºC and 240ºC preheat for 10s, respectively, and a 160ºC cut heat.

2.3. Equipment and equivalent dose determination

Following sample preparation, luminescence measurements were performed on a Risø TL/OSL-DA-20 reader (Bøtter-Jensen *et al.*, 2010) equipped with a 1.48 GBq ^{90}Sr-^{90}Y beta radiation source with a dose rate ~0.084 Gy/s. Quartz OSL was obtained through stimulating with blue LEDs emitting at 470 nm (FWHM = 20 nm) and delivering ~50 mW/cm^2 at the sample position and infrared (IR) stimulating using IR diodes emitting at 880 nm delivering ~145 mW/cm^2. Signals were detected using a 7 mm Hoya U-340 optical filter in front of an EMI 9235QA photomultiplier tube.

Measurements of OSL were made on chemically purified coarse-grained quartz, using the single-aliquot regenerative-dose (SAR) protocol proposed by Murray and Wintle (2003).

All OSL measurements were made using stimulation with blue diodes at 125°C for 40 s. To determine D_e, the initial 0.8 s (channels 1 to 5) of the OSL decay curve was used, and the background was assumed as the mean of the signal in the last 8 s (50 channels) of the 40 s measurement of the decay curve. Preheat temperatures of 240ºC for 10 s for sediment samples and 260ºC for 10 s for pottery samples, were chosen after performing preheat plateau tests and dose recovery tests using different preheat temperatures. A cut heat of 160ºC followed by immediate cooling prior to test dose response of approximately 5 Gy was used. Preliminary luminescence measurement tests on aliquots from the pottery samples, using the standard SAR protocol, were found to have significant recuperated corrected OSL signal compared to the natural signal (e.g. GyrOSL1_13, >10%). Thus, an additional 40 s optical stimulation at 280ºC was added at the end of each measurement cycle of the SAR protocol, and recuperation was reduced to <10% for all pottery samples.

The D_e values were calculated using the Analyst software (Duller, 2015) by fitting an exponential or exponential-plus-linear function to the dose-response curve, with an instrumental error of 1.0 %.

2.4. Dose rate assessment

The environmental dose rate for each sample was calculated using high-resolution gamma spectrometry to measure the radionuclide concentrations of ^{238}U, ^{232}Th and ^{40}K (Murray *et al.*, 1987), at the Nuclear Physics Laboratory of the University of Ioannina. Dry sample material was packed in plastic containers, sealed and stored at least for four weeks to allow for radon equilibrium before being measured on a Canberra broad energy HPGe gamma spectrometer for ~48h. The concentrations of ^{238}U, ^{232}Th and ^{40}K were then used to calculate the dose rates using the conversion factors of Adamiec and Aitken (1998) and Liritzis *et al.* (2013). The water content (% weight) of each sample was measured in the laboratory based on the initial field water content. In addition to the environmental dose rate, the contribution of the cosmic radiation was calculated based on the modern burial depth of the samples, the sediment density (1.8 g/cm^3) and the site's latitude, longitude and altitude, using the equations given by Prescott and Hutton (1994). The analytical results from gamma spectroscopy measurements are summarized in Table 1.

2.5. Luminescence characteristics

To establish appropriate preheat conditions for the SAR measurement protocol, preheat plateau tests and dose recovery tests using different preheat temperatures were conducted on representative samples. We first examined the dependence of D_e on different preheat temperatures, using representative samples selected to be studied in detail. In this experiment, twenty-four aliquots were measured for each sample (three aliquots for each preheat temperature) by the SAR protocol using eight different preheat temperatures from 160 to 300ºC (in 20ºC steps) for 10 s, with a fixed test dose cut heat temperature of 160ºC. For sample Gyr2OSL_07E, a plateau was detected between temperatures 180-300ºC, giving an average D_e of 5.58 ± 0.47 Gy. The recycling ratios and the signal recuperation values are all within 10% of unity and <2.0% of the natural signal, respectively. The D_e values of the sample Gyr1OSL_13 also show to be independent of preheat temperatures at least between 180 to 300ºC, giving an average D_e of 5.79 ± 1.10 Gy. The recycling ratios obtained are also within 10% of unity but the recuperation values are sufficiently high (3 - 13 %), in the temperature region 180 - 300ºC. High recuperation values of pottery samples can be attributed to low count rates of the natural OSL signal of the samples (Choi et al., 2009). In order to minimize this effect an additional 40 s optical stimulation at 280ºC was included as an extra step at the end of the SAR protocol (Murray and Wintle, 2003). A dose recovery test was also performed. Twenty-four aliquots from each sample were bleached by exposure to blue LED stimulation for 1 ks at room temperature (Rowan *et al.*, 2012), with a 10 ks pause between bleaches to allow charge in the 110ºC trap to empty, followed by another 1 ks blue LED stimulation. The aliquots were then given a beta dose of 5.60 Gy and were measured as if they were natural samples using the SAR protocol.

Measurements were made using a range of OSL preheat temperatures (160ºC - 300ºC, step 20ºC) using three aliquots for each temperature and a test dose cut heat of 160ºC. For sample Gyr2OSL_07E a plateau is identified between temperatures 160-300ºC and ratios of the recovered dose to given dose are within 10 % of unity for all temperatures. For sample Gyr1OSL_13 a plateau was identified between temperatures 180-280ºC, but the given dose seemed to be underestimated in the preheat temperature region between 160ºC and 240ºC. The recycling ratios for both samples were all within 10 % of unity, and signal recuperations were < 2.0 % of the natural signal. Based on these test results, a preheat temperature of 240ºC for sediment samples and 260ºC for pottery samples were adopted for all further SAR OSL measurements.

Table 1 - Sample information, radionuclide concentrations and dose rates results for luminescence samples collected from the two paleoseismological trenches at Gyrtoni Fault, Thessaly, Central Greece.

Sample no.	Sample position	Material	Depth (m)[a]	Water Content (%)[b]	^{238}U (Bq/kg)[c]	^{232}Th (Bq/kg)[c]	^{40}K (Bq/kg)[c]	External β dose rate (Gy/ka)[d]	External γ dose rate (Gy/ka)[d]	Cosmic dose rate (Gy/ka)[e]	Total dose rate (Gy/ka)[f]
Gyrtoni 1 trench											
Gyr1OSL_01	Upthrown block	Sediment	0.5	7.3	28.1 ± 1.3	16.3 ± 1.1	327.8 ± 25.3	0.98 ± 0.05	0.65 ± 0.02	0.21 ± 0.02	1.84 ± 0.06
Gyr1OSL_02	Upthrown block	Sediment	1.1	5.5	20.2 ± 0.9	12.7 ± 0.7	279.5 ± 20.0	0.82 ± 0.04	0.52 ± 0.02	0.18 ± 0.02	1.51 ± 0.05
Gyr1OSL_03	Upthrown block	Sediment	0.7	19.2	38.1 ± 1.5	30.3 ± 1.5	489.9 ± 34.6	1.29 ± 0.06	0.89 ± 0.03	0.19 ± 0.02	2.37 ± 0.07
Gyr1OSL_04	Upthrown block	Sediment	1.2	26.6	24.5 ± 1.2	31.6 ± 1.4	454.6 ± 32.2	1.05 ± 0.05	0.73 ± 0.02	0.18 ± 0.02	1.96 ± 0.06
Gyr1OSL_05	Upthrown block	Sediment	1.4	23.6	26.2 ± 1.1	21.5 ± 1.1	347.2 ± 23.8	0.87 ± 0.04	0.60 ± 0.02	0.17 ± 0.02	1.64 ± 0.05
Gyr1OSL_06	Upthrown block	Sediment	2.5	43.7	20.4 ± 0.8	21.7 ± 0.8	269.3 ± 18.0	0.58 ± 0.03	0.43 ± 0.01	0.15 ± 0.02	1.17 ± 0.03
Gyr1OSL_07	Fault zone	Sediment	1.8	17.1	20.0 ± 1.1	23.3 ± 1.2	349.3 ± 27.6	0.89 ± 0.05	0.61 ± 0.02	0.17 ± 0.02	1.67 ± 0.06
Gyr1OSL_08	Fault zone	Sediment	1.8	12.2	15.0 ± 0.9	19.0 ± 1.1	445.0 ± 30.7	1.05 ± 0.06	0.62 ± 0.03	0.17 ± 0.02	1.84 ± 0.07
Gyr1OSL_09	Fault zone	Sediment	2.2	14.9	29.4 ± 1.3	20.4 ± 1.1	369.6 ± 27.3	1.01 ± 0.05	0.68 ± 0.02	0.16 ± 0.02	1.85 ± 0.06
Gyr1OSL_10	Downthrown block	Sediment	0.7	12.6	29.1 ± 1.4	28.8 ± 1.4	499.3 ± 34.3	1.32 ± 0.07	0.87 ± 0.03	0.20 ± 0.02	2.38 ± 0.07
Gyr1OSL_11	Downthrown block	Pottery	0.7	13.8	28.9 ± 1.3	26.0 ± 1.3	498.2 ± 35.7	1.28 ± 0.07	0.83 ± 0.03	0.20 ± 0.02	2.31 ± 0.08
Gyr1OSL_12	Downthrown block	Pottery	1.0	9.7	27.2 ± 1.4	30.0 ± 1.6	504.2 ± 35.9	1.36 ± 0.07	0.89 ± 0.03	0.18 ± 0.02	2.43 ± 0.08
Gyr1OSL_13	Downthrown block	Pottery	1.0	14.6	33.0 ± 1.5	26.5 ± 1.4	505.9 ± 35.2	1.32 ± 0.07	0.86 ± 0.03	0.18 ± 0.02	2.37 ± 0.07
Gyr1OSL_14	Downthrown block	Pottery	1.0	13.5	26.2 ± 1.1	25.4 ± 1.1	512.1 ± 31.1	1.29 ± 0.06	0.81 ± 0.03	0.18 ± 0.02	2.28 ± 0.07
Gyr1OSL_15	Downthrown block	Pottery	2.0	16.5	29.8 ± 1.1	25.0 ± 1.1	464.5 ± 30.1	1.19 ± 0.05	0.78 ± 0.02	0.16 ± 0.02	2.13 ± 0.06
Gyrtoni 2 trench-East wall											
Gyr2OSL_01E	Upthrown block	Sediment	0.9	13.9	19.3 ± 0.4	25.5 ± 0.6	330.5 ± 3.3	1.00 ± 0.01	0.63 ± 0.01	0.19 ± 0.02	1.81 ± 0.02
Gyr2OSL_02E	Upthrown block	Sediment	1.8	14.0	22.0 ± 0.4	32.2 ± 0.5	344.4 ± 4.6	1.03 ± 0.01	0.73 ± 0.01	0.17 ± 0.02	1.92 ± 0.02
Gyr2OSL_03E	Upthrown block	Sediment	2.4	47.3	37.6 ± 0.6	53.5 ± 0.8	359.3 ± 4.1	1.02 ± 0.01	0.81 ± 0.01	0.15 ± 0.02	1.98 ± 0.02
Gyr2OSL_04E	Downthrown block	Sediment	0.8	11.4	20.3 ± 0.4	28.2 ± 0.6	434.1 ± 3.7	1.26 ± 0.01	0.76 ± 0.01	0.19 ± 0.02	2.21 ± 0.02
Gyr2OSL_05E	Downthrown block	Sediment	1.6	16.3	24.6 ± 0.4	26.3 ± 0.6	418.6 ± 3.7	1.20 ± 0.01	0.72 ± 0.01	0.17 ± 0.02	2.09 ± 0.02
Gyr2OSL_06E	Downthrown block	Sediment	2.4	34.9	26.5 ± 0.5	27.1 ± 0.6	418.7 ± 3.8	1.02 ± 0.01	0.63 ± 0.01	0.15 ± 0.02	1.81 ± 0.02
Gyr2OSL_07E	Downthrown block	Sediment	1.8	15.1	20.8 ± 0.4	26.3 ± 0.6	404.4 ± 3.6	1.15 ± 0.01	0.69 ± 0.01	0.17 ± 0.02	2.01 ± 0.02
Gyr2OSL_08E	Downthrown block	Sediment	1.4	13.4	30.1 ± 0.5	31.2 ± 0.6	436.4 ± 3.8	1.35 ± 0.01	0.85 ± 0.01	0.18 ± 0.02	2.38 ± 0.02
Gyr2OSL_09E	Downthrown block	Sediment	0.9	13.1	20.5 ± 0.4	29.8 ± 0.6	482.4 ± 4.0	1.35 ± 0.01	0.79 ± 0.01	0.19 ± 0.02	2.33 ± 0.02
Gyrtoni 2 trench-West wall											
Gyr2OSL_01W	Downthrown block	Sediment	2.4	24.6	20.4 ± 0.4	28.3 ± 0.5	399 ± 3.5	1.04 ± 0.01	0.65 ± 0.01	0.16 ± 0.02	1.85 ± 0.02

[a] Depth below the surface of the trench.
[b] Water content expressed as a percentage of the mass of dry sediment, calculated using field values.
[c] Concentrations of ^{238}U, ^{232}Th and ^{40}K were determined from laboratory measurements using high-resolution gamma spectrometry.
[d] Beta and gamma dose rates were calculated using the conversion factors of Adamiec and Aitken (1998) and are shown rounded to two decimal places, although the total dose rates were calculated using values prior to rounding. Dose rates have been corrected for the effect of the water content and grain size.
[e] Cosmic dose rates were calculated according to Prescott and Hutton (1994).
[f] Total dose rates were calculated after Aitken (1985).

Finally, in order to confirm the suitability of the chosen SAR protocol to accurately measure a known laboratory dose, dose-recovery tests have been performed on all samples (Murray and Wintle, 2003). During these tests, three new aliquots of each sample were bleached twice using the same procedure as previously described, and a known dose close to the expected natural dose (~De) was applied. The same preheating conditions and measurement sequence as selected for dating were used. Of 74 aliquots, ~85% had dose recovery ratios within the range 0.9 - 1.1. The statistical analysis of the doses recovered show a mean and standard deviation of 0.98 ± 0.06 of the given laboratory dose, confirming that the chosen SAR protocol is able to recover a given dose prior to any thermal treatment for all samples. The aliquots' measurements were accepted when the following criteria were satisfied: (i) recycling ratio of 1.0 ± 0.1, (ii) OSL-IR depletion ratio of 1.0 ± 0.1, (iii) a detectable OSL signal (i.e. >3 sigma above background), (iv) recuperation of signal less than 5% of the natural signal for soil samples and 10% for pottery samples, and (v) whether the sensitivity corrected natural signal intersected the dose-response curve.

Typical dose-response curves, for pottery sample (Gyr1OSL_13) sediment samples (Gyr2OSL_07E and Gyr1OSL_06), and natural OSL signal decay curves are shown in Fig. 2. The decay curves are typical for quartz, and show that the OSL signal was depleted rapidly during the initial 3 s of stimulation, indicating that the signal was dominated by the fast component. The dose-response curves of samples Gyr2OSL_07E and Gyr1OSL_13 were fitted by a single exponential function. The D_e values of 5.54 ± 0.17 Gy and 5.50 ± 0.34 Gy were obtained for these samples, respectively. The D_e values obtained are far below the saturation level of their growth curves except for the Gyr1OSL_06 sample. Although the D_e value of 285.2 ± 17.3 Gy that was obtained for this sample is in a dose range where the exponential component is saturated, the continuous growth of the dose-response curve indicates saturation at much higher doses.

2.6. Equivalent dose distribution

Sediment samples from depositional environments, such as floodplains and colluvial systems may not be well-bleached due to the short fluvial or gravity transport distance (Wallinga, 2002a). The D_e distribution of an insufficiently bleached sample is expected to have a scattered form and high overdispersion values (σ_{OD}) (Wallinga, 2002b). Overdispersion values >20% may indicate incomplete bleaching (Olley *et al.*, 2004).

Table 2 - Equivalent doses (De) and quartz OSL ages calculated for samples collected from the two paleoseismological trenches at Gyrtoni Fault, Thessaly, Central Greece.

Sample no.	Grain size (μm)	Aliquots (n)[a]	σ_{OD} (%)[b]	Total dose rate (Gy/ka)	Equivalent dose De (Gy) CAM[c]	Age (ka)[d] CAM
Gyrtoni 1 trench						
Gyr1OSL_01	125 - 250	27	33	1.84 ± 0.06	84.91 ± 5.36	46.1 ± 3.3
Gyr1OSL_02	125 - 250	28	19	1.51 ± 0.05	76.54 ± 2.90	50.5 ± 2.5
Gyr1OSL_03	125 - 250	16	17	2.37 ± 0.07	204.85 ± 10.14	86.4 ± 5.0
Gyr1OSL_04	125 - 250	20	11	1.96 ± 0.06	250.95 ± 7.00	128.3 ± 5.4
Gyr1OSL_05	125 - 250	27	13	1.64 ± 0.05	220.08 ± 6.34	133.9 ± 5.5
Gyr1OSL_06	125 - 250	24	21	1.17 ± 0.03	273.14 ± 12.56	233.3 ± 12.5
Gyr1OSL_07	125 - 250	25	30	1.67 ± 0.06	34.77 ± 2.12	20.9 ± 1.5
Gyr1OSL_08	125 - 250	22	30	1.84 ± 0.07	51.68 ± 3.44	28.1 ± 2.1
Gyr1OSL_09	125 - 250	32	26	1.85 ± 0.06	45.74 ± 2.13	24.7 ± 1.4
Gyr1OSL_10	125 - 250	43	17	2.38 ± 0.07	3.38 ± 0.09	1.42 ± 0.06
Gyr1OSL_11	125 - 250	50	18	2.31 ± 0.08	7.26 ± 0.19	3.15 ± 0.13
Gyr1OSL_12	125 - 250	17	29	2.43 ± 0.08	5.42 ± 0.44	2.23 ± 0.19
Gyr1OSL_13	125 - 250	41	11	2.37 ± 0.07	5.96 ± 0.13	2.52 ± 0.10
Gyr1OSL_14	125 - 250	41	13	2.28 ± 0.07	4.52 ± 0.11	1.98 ± 0.08
Gyr1OSL_15	125 - 250	42	12	2.13 ± 0.06	8.03 ± 0.16	3.77 ± 0.13
Gyrtoni 2 trench-East wall						
Gyr2OSL_01E	63 - 100	23	29	1.81 ± 0.02	167.9 ± 10.80	92.6 ± 6.1
Gyr2OSL_02E	100 - 150	20	24	1.92 ± 0.02	186.5 ± 12.40	96.9 ± 6.5
Gyr2OSL_03E	63 - 100	10	21	1.98 ± 0.02	293.6 ± 21.20	148.2 ± 10.8
Gyr2OSL_04E	63 - 100	24	16	2.21 ± 0.02	8.04 ± 0.26	3.64 ± 0.12
Gyr2OSL_05E	63 - 100	26	9	2.09 ± 0.02	7.28 ± 0.14	3.48 ± 0.07
Gyr2OSL_06E	63 - 100	25	6	1.81 ± 0.02	6.83 ± 0.09	3.77 ± 0.06
Gyr2OSL_07E	63 - 100	25	8	2.01 ± 0.02	5.62 ± 0.10	2.80 ± 0.06
Gyr2OSL_08E	63 - 100	26	5	2.38 ± 0.02	5.13 ± 0.05	2.16 ± 0.03
Gyr2OSL_09E	63 - 100	26	7	2.33 ± 0.02	3.14 ± 0.05	1.35 ± 0.02
Gyrtoni 2 trench-West wall						
Gyr2OSL_01W	63 - 100	25	9	1.85 ± 0.02	10.31 ± 0.21	5.59 ± 0.13

[a] n is the number of aliquots accepted for D_e calculations.
[b] σ_{OD} is the overdispersion of the D_e distribution.
[c] Equivalent doses (D_e) and OSL ages calculated using the central age model (CAM) of Galbraith et al. (1999).
[d] OSL ages are expressed as thousands of years (ka) before 2014 AD, and rounded to the nearest 100 years whith the exception of the relatively young samples which are rounded to the nearest 10 years.

The D_e distributions obtained for these samples are usually narrow and symmetrical with overdispersion values <20%, except for the pottery sample Gyr1OSL_12 which shows a significant overdispersion (29%) and a skewed D_e distribution (Table 2), indicating sufficient bleaching of the fluvio-colluvial sediments of the downthrown block of the GF. Therefore, the central age model (CAM; Galbraith and Roberts, 2012) was applied to the D_e data for all samples. The estimated D_e values for all samples are summarized in Table 2.

3. Results and discussion

3.1. OSL ages

The OSL ages were calculated by dividing the CAM D_e by the total dose rate. Table 2 summarizes the OSL chronology for the two excavated paleoseismological trenches at GF. The derived ages of the samples from the upthrown fault blocks of the two paleoseismological trenches are in stratigraphic order, within uncertainties. The six samples from the exposed four units on the upthrown block of trench G1 were dated between 46.1 ± 3.3 and 233.3 ± 12.5 ka (Table 2). The ages of the three samples dated from the displaced blocks of fifth upper unit ranged from 20.9 ± 1.5 ka to 28.1 ± 2.1 ka (Table 2), which nicely fit the stratigraphic order of this unit. Three additional samples were also dated from the units exposed on the upthrown fault block of trench G2 to check for internal consistency between trenches. These samples provided ages of 92.6 ± 6.1 ka (Gyr2OSL_01E), 96.9 ± 6.5 ka (Gyr2OSL_02E) and 148.2 ± 10.8 ka (Gyr2OSL_03E). Sample Gyr2OSL_01E showed comparable age, that agreed within one standard deviation, to the sample Gyr1OSL_03 (86.4 ± 5.0 ka) which was taken from the middle part of the same silty clay deposit of the trench G1. The sample Gyr2OSL_03E (148.2 ± 10.8 ka) collected from the base unit is in stratigraphic order with the samples Gyr1OSL_05 (133.9 ± 5.5 ka) and Gyr1OSL_06 (233.3 ± 12.5 ka) taken from the upper and the lower part, respectively, of the same massive silty clay unit exposed on trench G1.

In summary, all OSL ages from the upthrown fault block clearly document that the exposed units were deposited during the upper part of the Middle Pleistocene and mainly during the Late Pleistocene. Van Andel *et al.* (1990) estimated that the *Agia Sophia alluvium*, which is the earliest and most extensive unit of the *Niederterrasse*, deposited between c. 40 to 27 ka BP during the last glacial period, and is overlaid by a mature paleosoil (*Agia Sophia soil*). Interestingly, OSL ages from units 4 and 5 ranges from 50 to 21 ka thus suggesting they likely belong to the Agia Sophia alluvium (see Tsodoulos *et al.*, 2016).

A ceramic fragment (Gyr1OSL_15) from the buried pottery that was found on unit 6 (trench G1), was dated and provided an OSL age of 3.77 ± 0.13 ka (Table 2) with an archaeological estimation by the Department of History and Archaeology of the University of Ioannina (Dr. Andreas Vlachopoulos, personal communication) to be from 2000 – 1600 B.C. (Middle Bronze Age), thus in good agreement with the OSL age. The four pottery fragments dated from trench G1, provided OSL ages ranging from 1.98 ± 0.08 to 3.15 ± 0.13 ka (Table 2). The determined OSL ages for the pottery fragments were expected to be older than the ages of the sediment unit in which they were found (Moro *et al.*, 2013; Vanneste *et al.*, 2006). This is consistent with the OSL age (1.42 ± 0.06 ka) of the sediment sample Gyr1OSL_10 taken from the base of unit 7 (trench G1, see Tsodoulos *et al.*, 2016) (Table 2). In trench G2, the calculated OSL ages for unit 5 ranged from 1.35 ± 0.02 to 3.77 ± 0.06 ka (Table 2). Samples Gyr2OSL06E to 09E were collected in a vertical sequence at every ~0.50 m. Thus, from the obtained OSL ages of these samples a mean age trend with depth of 1.60 yr/cm and a mean sedimentation rate of 0.62 mm/yr was estimated. An OSL age of 5.59 ± 0.13 ka was obtained for a sediment sample (Gyr2OSL_01W) from the scarp derived colluvial deposit (unit 4), west wall in trench G2 (see Tsodoulos *et al.*, 2016) (Table 2). Overall, the calculated OSL ages indicate that the fluvial-colluvial deposits of the downthrown fault block were deposited during the Middle-Late Holocene. Previous researchers (Demitrack, 1986) consider the *Gyrtoni alluvium* to have been deposited between c. 5.0 and 4.0 ka BP, using archaeological criteria, and defined the end of the deposition of the higher floodplain of the Pinios River.

4. Conclusions

The OSL characteristics of the studied samples from the two paleoseismological trenches were discussed. Recycling ratio, recuperation and dose recovery tests confirmed the suitability of the quartz grains for OSL dating purposes, using the SAR protocol. Preheat plateau tests were also performed to select the appropriate preheat temperatures. Overdispersion values of the assessed ages for each sample were found to be less than ~20% for the majority of the samples, indicating well bleached quartz and assuring the quality of the dating process. Using a combination of OSL dating and paleoseismological trenching, we have estimated dates of the observed paleoarthquakes related with the Gyrtoni Fault. The two paleoseismological trenches provide evidence of at least three, and possibly four faulting events (age ranges of 2.16-1.42 ka, 3.77-2.80 ka, 5.59-3.77 ka, and <5.59 ka) with an average recurrence interval 1.39 ± 0.14 ka. The estimated OSL ages agreed well with the available stratigraphical data, and archaeological evidence.

5. Acknowledgements

This research project was implemented within the framework of the Action «Supporting Postdoctoral Researchers» of the Operational Program "Education and Lifelong Learning" and is co-financed by the European Social Fund (ESF) and the Greek State.

6. References

Adamiec, G. and Aitken, M.J., 1998. Dose-rate conversion factors: update, *Ancient TL*, 16, 37-49.

Aitken, M.J., 1998. An Introduction to Optical Dating. Oxford University Press, Oxford.

Bøtter-Jensen, L., Thomsen, K.J. and Jain, M. 2010. Review of optically stimulated luminescence (OSL) instrumental developments for retrospective dosimetry, *Radiation Measurements*, 45, 253-257.

Bronk Ramsey, C., 1995. Radiocarbon calibration and analysis of stratigraphy: the OxCal program, *Radiocarbon*, 37(2), 425-430.

Caputo, R. and Helly, B., 2005a. The Holocene activity of the Rodia Fault, Central Greece, *Journal of Geodynamics*, 40(2-3), 153-169.

Caputo, R., Helly, B., Pavlides, S. and Papadopoulos, G., 2004. Palaeoseismological investigation of the Tyrnavos Fault (Thessaly Central Greece), *Tectonophysics*, 394, 1-20.

Caputo, R., Helly, B., Pavlides, S. and Papadopoulos, G., 2006. Archaeo- and palaeoseismological investigations in Northern Thessaly (Greece): Insights for the seismic potential of the region, *Natural Hazards*, 39, 195-212.

Chatzipetros, A., Pavlides, S. and Mountrakis, D., 1998. Understanding the 13 May 1995 western Macedonia earthquake: a paleoseismological approach, *Journal of Geodynamics*, 26, 327-339.

Chen, Y.G., Chen, Y.W., Chen, W.S., Zhang, J.F., Zhaoc, H., Zhou, L.P. and Li, S.H., 2003. Preliminary results of long-term slip rates of 1999 earthquake fault by luminescence and radiocarbon dating, *Quaternary Science Reviews*, 22, 1213-1221.

Choi, J.H., Kim, J.W., Murray, A.S., Hong, D.G., Change, H.W. and Cheong, C.-S., 2009. OSL dating of marine terrace sediments on the southeastern coast of Korea with implications for Quaternary tectonics, *Quaternary International*, 199, 3-14.

Constantin, D., Begy, R., Vasiliniuc, S., Panaiotu, C., Necula, C., Codrea V. and Timar-Gabor, A., 2014. High-resolution OSL dating of the Costines¸ ti section (Dobrogea, SE Romania) using fine and coarse quartz, *Quaternary International*, 334-335, 20-29.

Demitrack, A., 1986. The Late Quaternary geologic histoty of the Larissa Plain, Thessaly, Greece: Tectonic, Climatic and Human Impact on the Landscape, Ph .D. dissertation, Stanford University, CA. Ann Arbor, Michigan: University Microfilms.

Duller, G.A.T., 2003. Distinguishing quartz and feldspar in single grain luminescence measurements, *Radiation Measurements*, 37, 161-165.

Duller, G.A.T., 2015. The Analyst software package for luminescence data: overview and recent improvements, *Ancient TL*, 33(1), 35-42.

Fattahi, M., Nazari, H., Bateman, M.D., Meyere, B., Sébrier, M., Talebian, M., Le Dortz, K., Foroutan, M., Ahmadi Givi, F. and Ghorashi, M., 2010. Refining the OSL age of the last earthquake on the Dheshir fault, Central Iran, *Quaternary Geochronology*, 5(2-3), 286-292.

Galbraith, R.F. and Roberts, R.G., 2012. Statistical aspects of equivalent dose and error calculation and display in OSL dating: an overview and some recommendations, *Quaternary Geochronology*, 11, 1-27.

Huntley, D.J., Godfrey-Smith, D.I. and Thewalt, M.L.W., 1985. Optical dating of sediments, *Nature*, 313, 105-107.

Liritzis, I., Stamoulis, K., Papachristodoulou, C. and Ioannides, K., 2013. A re-evaluation of radiation dose-rate conversion factors, *Mediterr. Archaeol. Archaeom*., 13, 1-15.

McCalpin, J.P., 2009a. Field techniques in paleoseismology. Paleoseismology in extensional tectonic environments. *In*: McCalpin, J.P., *eds*., *Paleoseismology*, Academic Press, San Diego, 161-269.

McCalpin, J.P., 2009b. Application of Paleoseismic Data to Seismic Hazard Assessment and Neotectonic Research. *In*: McCalpin, J.P., *eds*., *Paleoseismology,* Academic Press, San Diego, 1-106.

Moro, M., Gori, S., Falcucci, E., Saroli, M., Galadini, F. and Salvi, S., 2013. Historical earthquakes and variable kinematic behaviour of the 2009 L'Aquila seismic event (central Italy) causative fault, revealed by paleoseismological investigations, *Tectonophysics*, 583, 131-144.

Murray, A.S., Marten, R., Johnston, A. and Martin, P., 1987. Analysis for naturally occurring radionuclides at environmental concentrations by gamma spectrometry, *Journal of Radioanalytical and Nuclear Chemistry*, 115, 263-288.

Murray, A.S. and Olley, J.M., 2002. Precision and accuracy in the optically stimulated luminescence dating of sedimentary quartz, *Geochronometria*, 21, 1-16.

Murray, A.S. and Wintle, A.G., 2003. The single aliquot regenerative dose protocol: potential for improvements in reliability, *Radiation Measurements*, 37, 377-381.

Olley, J.M., Pietsch, T. and Roberts, R.G., 2004. Optical dating of Holocene sediments from a variety of geomorphic setting using single grains of quartz, *Geomorphology*, 60, 337-358.

Pavlides, S., Caputo, R., Sboras, S., Chatzipetros, A., Papathanasiou, G. and Valkaniotis, S., 2010. The Greek catalogue of active faults and database of seismogenic sources, *Bulletin of the Geological Society of Greece*, XLIII/1, 486-494.

Papazachos, B.C. and Papazachou, C., 1997. The Earthquakes of Greece, Editions ZITI, Thessaloniki.

Porat, N., Wintle, A.G., Amit, R. and Enzel, Y., 1996. Late Quaternary earthquake chronology from luminescence dating of colluvial and alluvial deposits of the Arava Valley, Israel, *Quaternary Research*, 46, 107-117.

Prescott, J.R. and Hutton, J.T., 1994. Cosmic ray contribution to dose rates for luminescence and ESR dating: large depths and long-term time variations, *Radiation Measurements,* 23, 497-500.

Rowan, A.V., Roberts, H.M., Jones, M.A., Duller, G.A.T., Covey-Crump, S.J. and Brocklehurst, S.H., 2012. Optically stimulated luminescence dating of glaciofluvial sediments on the Canterbury Plains, South Island, New Zealand, *Quaternary Geochronology*, 8, 10-22.

Tsodoulos, I., Chatzipetros, A., Koukouvelas, I., Caputo, R., Pavlides, S., Stamoulis, K., Gallousi, C., Papachristodoulou, C., Belesis, A., Kalyvas, D. and Ioannides, K., 2016. Palaeoseismological investigation of the Gyrtoni Fault (Thessaly, Central Greece), *Submitted for the proceedings of the 14th Intern. Conference*, Thessaloniki, May 2016.

Van Andel, T.H., Zangger, E. and Demitrack, A., 1990. Land use and soil erosion in prehistoric and historical Greece, *J. Field Archaeology*, 17, 379-376.

Vanneste, K., Radulov, A., De Martini, P., Nikolov, G., Petermans, T., Verbeeck, K., Camelbeeck, T., Pantosti, D., Dimitrov, D. and Shanov, S., 2006. Paleoseismologic investigation of the fault rupture of the 14 April 1928 Chirpan earthquake (M 6.8), southern Bulgaria, *J. Geophys. Res*., 111, B01303.

Wallinga, J., 2002a. Optically stimulated luminescence dating of fluvial deposits: a review, *Boreas*, 31, 303-322.

Wallinga, J., 2002b. Detection of OSL age overestimation using single-aliquot techniques, *Geochronometria*, 21, 17-20.